WPMAG-CPR(17) 17869

M. Lewandowska et al.

# Experimental study of steady-state transverse heat transfer in a single channel CICC

Preprint of Paper to be submitted for publication in Proceeding of 13th European Conference on Applied Superconductivity

This work has been carried out within the framework of the EUROfusion Consortium and has received funding from the Euratom research and training programme 2014-2018 under grant agreement No 633053. The views and opinions expressed herein do not necessarily reflect those of the European Commission.

# Experimental study of steady-state transverse heat transfer in a single channel CICC

Monika Lewandowska, Aleksandra Dembkowska and Leszek Malinowski

***Abstract*—A new configuration of the THETIS installation (for thermal-hydraulic tests of forced-flow superconducting cables, such as e.g. Cable-in-Conduit Conductors (CICCs), has been prepared at West Pomeranian University of Technology, Szczecin. In the present form THETIS enables pressure drop and heat transfer coefficient measurements in short samples of conductors using water in a wide range of temperature and Reynolds number. We present the new configuration of the installation and demonstrate its capabilities by reporting the results of the first thermal-hydraulic test conducted on a smooth tube with a square cross section and on a reference sample (JT-60SA TF conductor). The results obtained for a smooth tube are in good agreement with predictions of the standard Dittus-Boelter heat transfer correlation, which positively verifies correctness of the applied procedures. The experimental Nu values obtained for the CICC sample remain almost constant in the considered Re range 700 – 1700, and they are about 3 times larger than those predicted by the smooth tube correlation.**

***Index Terms*—heat transfer coefficient, forced-flow superconducting cables, CICC, THETIS.**

## I. Introduction

PRESENT models used in thermal–hydraulic analyses of forced-flow superconducting cables, such as e.g. Cable-in-Conduit Conductors (CICCs), are most often 1-D and they need accurate predictive correlations for the transverse mass, momentum- and energy transport processes between the different cable components, in order to reliably analyze any superconducting magnet design in both normal operating conditions and off-normal conditions (e.g. during quench evolution) [1], [2]. Very few heat transfer correlations for flow in a CICC bundle have been proposed in literature [3]-[5], but none of them is commonly accepted for predictive use. As a result, in thermal-hydraulic analyses of the designs of the DEMO coils [6]-[13] classical heat transfer correlations for flows in smooth tubes are used, which are undoubtedly over-conservative in these cases. The existing experimental database of heat transfer coefficients in a CICC bundle is also very modest [14]. There is a need to perform systematic measurements of heat transfer coefficients in a CICC bundle, which could serve as a base for further attempts to develop predictive correlations.

The THETIS installation for thermal-hydraulic tests of forced-flow superconducting cables, such as e.g. CICCs, has been prepared at West Pomeranian University of Technology, Szczecin. The aim of the paper is to present the THETIS final configuration and to report the results of the first performed measurements of the transverse heat transfer coefficient in a short reference CICC sample (JT-60SA TF conductor).

## II. Experimental Setup

### A. THETIS installation

The THETIS basic configuration, which allowed pressure drop tests of superconducting cables using distilled water at room temperature, is described in detail in [15]. Recently, THETIS has been upgraded, by adding a main heater and an air flow cooler, which enable adjustments of the water temperature in the circuit in the range from room temperature to 70ºC. The hydraulic scheme of the new THETIS configuration is presented in Fig. 1.

### B. Samples characteristics and instrumentation

To verify correctness of the applied test procedure the first trial THETIS measurement of the transverse heat transfer coefficient between the flowing fluid and the wall was conducted using a smooth tube with a square cross section. Then similar test of the JT60-SA TF (JTF091 sample) single channel Cable-in-Conduit Conductor (CICC) sample was performed. The parameters of these samples relevant for the present study are given in Table I, whereas the full characteristics of the JT-60SA TF conductor can be found in [16],[17].

Schemes of the samples' instrumentation are shown in Fig. 2. Water temperature at the sample inlet and outlet, $T_{in}$ and $T_{out}$, was measured with two temperature sensors T-111-6-115-60-3-G1/2-NA-A-Pt1000-400 with accuracy ± 0.15 ºC ± 0.2%·|$t$|. The same kind of temperature sensors was used to

TABLE I
Characteristics of the JT-60SA TF (JTF091) sample [16],[17] and the smooth tube used in the experiment

| Quantity, unit | Symbol | Smooth tube | CICC |
|---|---|---|---|
| Inner dimensions, mm × mm | $x \times y$ | 21 × 21 | 18 × 22 |
| Void fraction, % | $\varphi$ | 100 | 32 |
| Flow area, mm$^2$ | $A_f$ | 440 | 126 |
| Hydraulic diameter, mm | $D_h$ | 21.3 | 0.454 |
| Wall thickness, mm | $t_w$ | 2 | 2 |

This work was carried out within the framework of the EUROfusion Consortium and was supported in part by the Euratom Research and Training Program 2014–2018 under Grant 633053 and in part by the Polish Ministry of Science and Higher Education within the framework of the financial resources in the year 2017 allocated for the realization of the international cofinanced project.

M. Lewandowska, A. Dembkowska and L. Malinowski are with the West Pomeranian University of Technology, Szczecin, 70-310 Szczecin, Poland (e-mail: monika.lewandowska@zut.edu.pl).

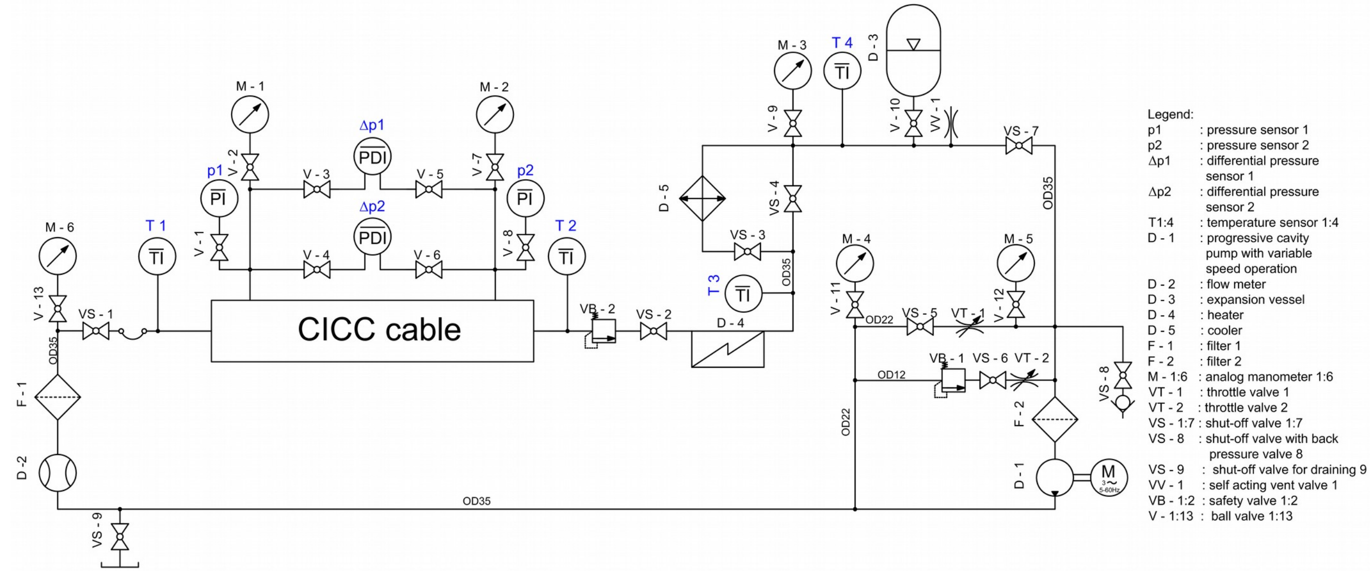


Fig. 1. Hydraulic scheme of the new configuration of the THETIS installation.

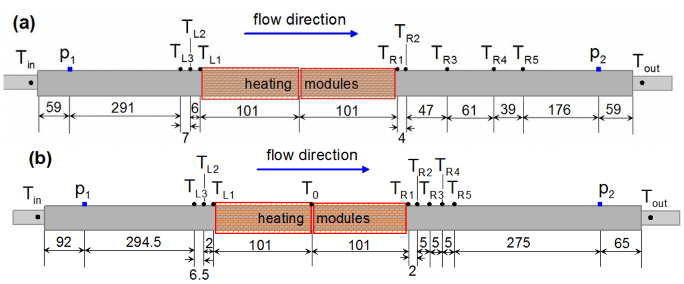


Fig. 2. Instrumentation scheme of the (a) smooth tube, (b) CICC sample, not in scale. Dimensions in mm.

control the water temperature at the outlets of the main heater and the cooler. Water pressure in the sample, $p_1$ and $p_2$, was measured with the pressure sensors Aplisens PR-28/0-25BAR/ M20x1.5 and Aplisens PR-28/0-10BAR/ M20x1.5, respectively, with accuracy ± 0.2% of measuring range. The mass flow rate was measured with the flow meter KROHNE OPTIMASS 1000. Two heating modules, each of length 0.100 m, and several Platinum Resistance Temperature Detectors Pt1000, Class DIN 1/3B, with accuracy: ± 0.1 ºC ± 0.17%·|$t$| were attached at the outer surface of the sample. Each heating module consisted of 4 thin copper plates. Each copper plate was fully covered with 4 square resistive foil heaters (25 mm × 25 mm, nominal power 40 W). After installing the heating modules and temperature sensors the sample was wrapped with a thermal insulation tape. A photo of the CICC sample without the thermal insulation is shown in Fig. 3.

### C. Test procedure

At a set mass flow rate we adjusted the initial temperature in the circuit at 41.2 ºC and 41.4 ºC for the smooth tube and for the CICC sample, respectively. After the steady state was reached we switched on the heating modules at the sample and slightly reduced the heating power of the main heater to keep constant temperature at the sample inlet and waited until the steady state was reached again. Then the heating modules

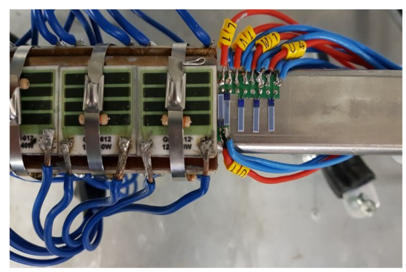

Fig. 3. Photo of a piece of the instrumented CICC sample without the thermal insulation showing the part of the right heating module and the temperature sensors $T_{R1} - T_{R5}$.

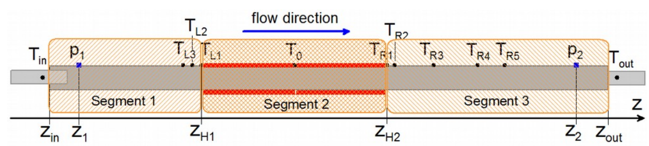


Fig. 4. Scheme of the considered system.

were switched off, and the whole procedure was repeated for next value of the mass flow rate. In the course of the experiment readings of the flow meter and of all the temperature and pressure sensors were registered in 1 s intervals by the Data Acquisition System. The average values and their standard deviations were computed for the data collected during steady states.

## III. Heat Transfer Analysis

Our analysis is based on the energy balance equations. We took into account the dependence of the water enthalpy on pressure and temperature. The sample length is divided into three segments as shown in Fig. 4. The pressure at the points $z_1$ and $z_2$ was read from the experimental data, and the pressure profile along the sample, $p(z)$, was obtained under the assumption that the pressure gradient in the sample was constant. The energy balance equations for the Segments 1-3, respectively, can be written as:

$$\dot{m}\left[i(p_{H1},T_{H1})-i(p_{in},T_{in})\right]=\dot{Q}_{c1}-\dot{Q}_{amb1} \quad , \tag{1a}$$

$$m\left[i(p_{H2},T_{H2})-i(p_{H1},T_{H1})\right]=Q_H-Q_{c1}-Q_{c3}-Q_{amb2} \quad , \tag{1b}$$

$$m\left[i(p_{out},T_{out})-i(p_{H2},T_{H2})\right]=Q_{c3}-Q_{amb3} \quad , \tag{1c}$$

where $m$ is the mass flow rate, $i$ is the water specific enthalpy, $Q_H$ is the thermal power released by the heating modules, $Q_{amb\ j}$ is the heat loss to ambient from the $j$-th Segment, and $Q_{c\ j}$ is the longitudinal heat transfer from the Segment 2 to the $j$-th Segment due to conduction in the wall. The value of $Q_H$, equal to 1201 W for the smooth tube and 1038 W for the CICC sample, was obtained based on measurements of voltage and resistance with accuracy 5%. We approximated the outer surface temperature profiles in the Segment 1 and 3, respectively, by the functions:

$$T(z)=T_{ref}(z)+A_1\exp\left[(z-z_{H1})/\lambda_1\right] \quad \text{for} \quad z_{in}\le z<z_{H1} \tag{2a}$$

$$T(z)=T_{ref}(z)+\Delta T_{out}+A_2\exp\left(\frac{z_{H2}-z}{\lambda_2}\right)+A_3\exp\left(\frac{z_{H2}-z}{\lambda_3}\right) \quad \text{for} \quad z_{H2}<z\le z_{out} \tag{2b}$$

where $z$ is the coordinate along the sample, $z_{H1}$ and $z_{H2}$ are the coordinates of the left and right boundary of the heated section (Segment 2), see Fig. 4, $\Delta T_{out} = T_{out}(Q_H) - T_{out}(0)$, and

$$T_{ref}(z)=T_{in}+\alpha_{JT}\left(p(z)-p_{in}\right) \quad , \tag{2c}$$

where $\alpha_{JT}$ = - 0.021145 K/bar is the Joule - Thomson coefficient. The values of parameters $A_1$ and $\lambda_1$ were obtained by least square fitting of Eq. (2a) to the readings of the sensors $T_{L1}$ - $T_{L3}$. Analogously we obtained the values of $A_2$, $\lambda_2$, $A_2$ and $\lambda_2$ using Eq. (2b) and the readings of $T_{R1}$ – $T_{R5}$. We assumed that at a large distance from the heated section the wall temperature should be equal to the water temperature. The temperature profile within the heated section ( $z_{H1}\le z\le z_{H2}$ ) was obtained by linear spline interpolation using the readings of temperature sensors $T_{L1}$, $T_0$ and $T_{R1}$. An example of the calculated temperature profile along the sample is presented in Fig. 5. We estimated the values of $Q_{c1}$ and $Q_{c3}$ at the boundaries of Segment 2 using the temperature profiles in the wall (Eqs. (2a) and (2b)) and the Fourier law of conduction.

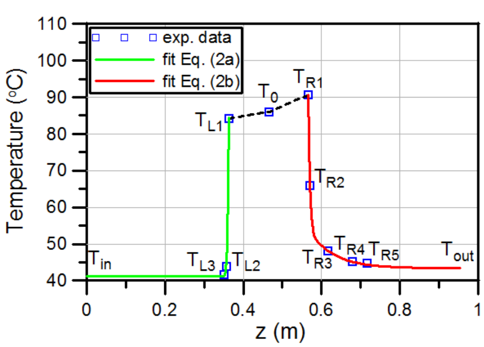


Fig. 5. Typical computed temperature profile along the smooth tube sample.

The average temperature of the outer surface of the $j$-th Segment wall was calculated as:

$$T_{wo\,j}=\left[\int_{z_{jR}}^{z_{j\,L}} T(z)\,dz\right]\text{¿}\left(z_{j\,R}-z_{j\,L}\right) \quad , \tag{3}$$

where $z_{jL}$ and $z_{jR}$ are the coordinates of the left and right boundary of the $j$-th Segment.

The heat rate transferred to the fluid, $Q_f$, and the total heat loss to ambient, $Q_{amb}$, were calculated as:

$$Q_f=m\left[i(p_{out},T_{out})-i(p_{in},T_{in})\right] \quad , \tag{4}$$

$$Q_{amb}=Q_{amb1}+Q_{amb2}+Q_{amb3}=Q_H-Q_f \quad . \tag{5}$$

The ratio of heat losses to ambient from the Segments 1 and 3 was expressed as:

$$\frac{Q_{amb1}}{Q_{amb3}}=\frac{S_{wo1}(T_{wo1}-T_{amb})}{S_{wo3}(T_{wo3}-T_{amb})} \quad , \tag{6}$$

where $S_{wo\ j}$ is the area of the outer surface of the $j$-th Segment wall and $T_{amb}$ is the ambient temperature. The system of equations (1a)-(1c), (5) and (6) was solved for the unknown $T_{H1}$, $T_{H2}$, $Q_{amb1}$, $Q_{amb2}$ and $Q_{amb3.}$ The average temperature of the inner surface of the 2nd Segment wall, $T_{wi2}$, was estimated from the Fourier law by solving the equation:

$$\frac{Q_H-Q_{c1}-Q_{c3}-Q_{amb2}}{S_{w\,av2}}=k_{steel}\frac{T_{wo2}-T_{wi2}}{t_w} \quad , \tag{7}$$

where $k_{steel}$ is the steel thermal conductivity and $S_{w\ av2}$ is the average area of the 2nd Segment wall. Finally, the heat transfer coefficient $h_{exp}$ was obtained by solving the equation

$$Q_H-Q_{c1}-Q_{c3}-Q_{amb2}=h_{\exp}S_{wi2}\left(T_{wi2}-T_f\right) \quad , \tag{8}$$

where $S_{wi2}$ is the area of the inner surface of the 2nd Segment wall and $T_f = (T_{H1} + T_{H2})/2$ is the average fluid temperature in the Segment 2. We also calculated the Nusselt number:

$$Nu_{exp}=h_{\exp}D_h/k_{water}(p_f,T_f) \quad , \tag{9}$$

where $p_f = (p_{H1} + p_{H2})/2$ is the reference pressure in the Segment 2.

## IV. Results and Discussion

The results of our analysis in dimensional and dimensionless form are presented in Figs. 6 and 7, respectively. For comparison we also added in Figs. 6 and 7 heat transfer coefficient and Nu values obtained with standard smooth tube correlations, i.e.: $Nu_{lam} = 4.364$ for the laminar flow and Dittus-Boelter correlation $Nu_{DB} = 0.023Re^{0.8}Pr^{0.4}$ for the turbulent flow. The Prandtl number value, calculated for

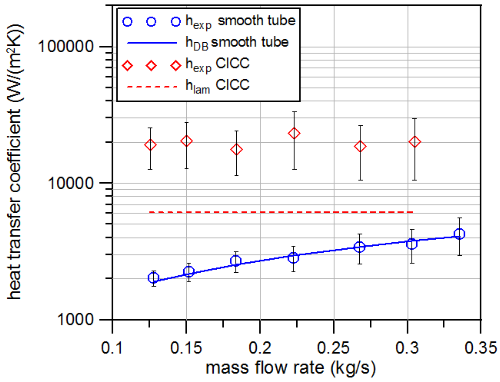


Fig. 6. Measured and calculated heat transfer coefficient as a function of mass flow rate.

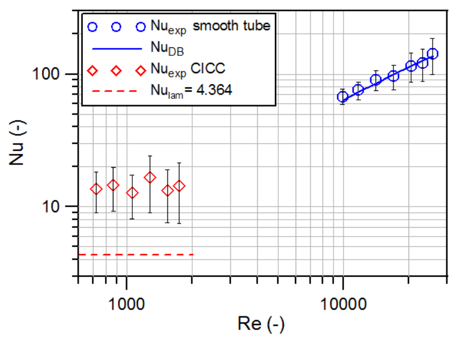


Fig. 7. Measured and calculated Nusselt number as a function of Reynolds number

each experimental point at the reference conditions ($p_f$, $T_f$), varied in the range 4.12 - 4.17, so it may be considered almost constant. It is seen in Figs. 6 and 7, that the experimental values of the heat transfer coefficient and Nu for the smooth tube agree well with the predictions of the Dittus-Boelter correlation, which positively verifies correctness of the applied test and analysis procedures. The values of the heat transfer coefficient for the smooth tube increase with the mass flow rate, whereas for the CICC remain at the constant level of about 20 000 W/(m$^2$K) within the whole considered mass flow rate range. Although the measurements for the smooth tube and for the CICC sample were performed in the similar mass flow rate ranges, the corresponding Re ranges for both samples are very different – the experimental Re range for the CICC sample falls in the laminar regime, whereas for the smooth tube in the turbulent regime. This effect results from much different values of hydraulic diameters of both samples. The values of the heat transfer coefficient and the respective $Nu_{exp}$ values for the CICC are about 3 times larger than the predictions of the smooth tube correlation. These results is consistent with those obtained by Wachi *et al.* in [14].

The uncertainties of $h_{exp}$ and $Nu_{exp}$ values are rather large – for the CICC they are of about 35-40%, which is not quite satisfactory. The main contribution to the total error bar of $h_{exp}$ and $Nu_{exp}$ is due to large uncertainty of $Q_f$ (see Eq. (4)), which results from the small increase of the fluid temperature within the sample – typical values of $\Delta T = T_{out} - T_{in}$ vary in the range 0.9 – 2 K, which cannot be measured very accurately with our thermometers. In further experiments we are going to add at least one more heating module to achieve larger values of $T_{out}$, which should result in reduction of $h_{exp}$ and $Nu_{exp}$ error bars.

## V. Summary Conclusions and Perspectives

The new configuration of the THETIS installation for thermal-hydraulic tests of forced-flow superconducting cables, using water at various temperatures, has been assembled. The first measurements of the transverse heat transfer coefficient between the wall and the fluid were performed in the smooth tube and in the CICC sample. The results obtained for the smooth tube agree well with predictions of the standard Dittus-Boelter correlation, which positively verified correctness of the applied procedures. The experimental values of the heat transfer coefficient remain at the constant level in the considered Re range 700-1700, and they are about 3 times larger than those predicted by the smooth tube correlation for the laminar flow. Further systematic measurements of the heat transfer coefficient at different values of the water inlet temperature are planned to obtain the results in a wide range of Pr and Re numbers.

## Acknowledgment

The views and opinions expressed herein do not necessarily reflect those of the European Commission.

## References

[1] R. Zanino and L. Savoldi Richard, "A review of thermal-hydraulic issues in ITER cable-in-conduit conductors," *Cryogenics*, vol. 46, 2006, pp. 541-545.

[2] R. Zanino, " Multiscale Approach and Role of Validation in the Thermal-Hydraulic Modeling of the ITER Superconducting Magnets," *IEEE Trans. Appl. Supercond.*, vol. 23, no. 3, Jun. 2013, Art. no. 4900607

[3] S. Nicollet, D. Ciazynski, J.-L. Duchateau, B. Lacroix and B. Renard, "Evaluation of the ITER cable-in-conduit-conductor heat transfer," Proceedings of the 20th ICEC, Beijing, China, Elsevier Ltd; 2005, pp. 589–92.

[4] L. Bottura and C. Marinucci, "A porous medium analogy for the helium flow in CICC's," *Int. J. Heat Mass Transfer*, vol. 51 , pp. 2494–2505, 2008.

[5] M. Lewandowska and L. Malinowski, "Transverse heat transfer coefficient in the dual channel ITER TF CICCs. Part III: Direct method of assessment," *Cryogenics*, vol. 73 (2016) 91-100.

[6] M. Lewandowska, K. Sedlak, "Thermal-Hydraulic Analysis of LTS Cables for the DEMO TF Coil," *IEEE Trans. Appl. Supercond.*, vol. 24, no. 3, Jun. 2014, Art. No. 4200305.

[7] M. Lewandowska and K. Sedlak, "Thermal-hydraulic analysis of the improved LTS conductor design concepts for the DEMO TF coil," *Prz. Elektrotech.*, vol. 92, no. 4, 2016, pp. 179–182.

[8] M. Lewandowska, K. Sedlak and L. Zani, "Thermal-hydraulic analysis of the low-$T_c$ Superconductor (LTS) winding pack design concepts for the DEMO Toroidal Field (TF) coil," *IEEE Trans. Appl. Supercond.*, vol. 26, no. 4, Jun. 2016, Art. No. 4205305.

[9] R. Zanino et al., "Development of a Thermal-Hydraulic Model for the European DEMO TF Coil," IEEE Trans. Appl. Supercond., vol. 26, no. 4, Jun. 2016, Art. no. 4201606.

[10] R. Zanino, R. Bonifetto, L. Savoldi and L. Muzzi, "4C Code Analysis of High-Margin Quench Propagation in a DEMO TF Coil," Proceedings of the IEEE 26th Symposium on Fusion Engineering (SOFE), DOI: 10.1109/SOFE.2015.7482374.

[11] R. Vallcorba et al., “Thermo-hydraulic analyses associated with a CEA design proposal for a DEMO TF conductor,” *Cryogenics*, vol. 80, 2016, pp. 317–324.
[12] K. Sedlak, P. Bruzzone and M. Lewandowska, “Thermal-hydraulic and quench analysis of the DEMO toroidal field winding pack WP1,” *Fus. Eng. Des.*, to be published.
[13] A. Dembkowska and M. Lewandowska, “Thermal-Hydraulic Analysis of the DEMO CS coil,” *IEEE Trans. Appl. Supercond.*, submitted for publication.
[14] Y. Wachi, M. Ono and T. Hamajima, “Heat Transfer Characteristics of the Supercritical Helium in a Cable-in-conduit Conductor,” *IEEE Trans. Appl. Supercond.*, vol. 5, no. 2, Jun. 1995, pp. 568-571.
[15] M. Lewandowska, W. Rachtan, A. Dembkowska, Malinowski, L. Zani, “Experimental stand for thermal-hydraulic tests of forced flow conductors using water at room temperature,” *Fus. Eng. Des.*, to be published.
[16] L. Zani, P. Barabaschi and M. Peyrot, “Starting EU Production of Strand and Conductor for JT-60SA Toroidal Field Coils,” *IEEE Trans. Appl. Supercond*., vol. 22, no. 3, Jun. 2012, Art. no. 4801804.
[17] P. Decool, et.al., “JT-60SA TF Coils: Experimental Check of Hydraulic Operating Conditions, *IEEE Trans. Appl. Supercond*., vol. 26, no. 4, Jun. 2016, Art. no. 4201705.